Spin-polarized tunneling as a probe of the electronic properties of $Ga_{1-x}Mn_xAs$ heterostructures

M. Elsen,[1,*] H. Jaffrès,[1] R. Mattana,[1] L. Thevenard,[2] A. Lemaitre,[2] and J.-M. George[1,†]
[1]*Unité Mixte de Physique CNRS/Thales, Route Départementale 128, 91767 Palaiseau Cedex, France and Université Paris-Sud 11, 91405 Orsay, France*
[2]*Laboratoire de Photonique et de Nanostructures, CNRS, Route de Nozay, 91460 Marcoussis, France*
(Received 27 April 2007; revised manuscript received 17 July 2007; published 11 October 2007; corrected 23 October 2007)

We present magnetic and tunnel transport properties of (Ga,Mn)As/(In,Ga)As/(Ga,Mn)As structure before and after adequate annealing procedure. The conjugate increase of magnetization and tunnel magnetoresistance obtained after annealing is shown to be associated with the increase of both exchange energy Δ_{exch} and hole concentration by reduction of the Mn interstitial atom in the top magnetic electrode. Through a 6×6 band $k\cdot p$ model, we established general phase diagrams of tunneling magnetoresistance (TMR) and tunneling anisotropic magnetoresistance (TAMR) vs (Ga,Mn)As Fermi energy (E_F) and spin-splitting parameter (B_G). This allows us to give a rough estimation of the exchange energy $\Delta_{exch}=6B_G\simeq-120$ meV and hole concentration of the order of $p=1\times10^{20}$ cm^{-3} for (Ga,Mn)As and beyond gives the general trend of TMR and TAMR vs the selected hole band involved in the tunneling transport.

DOI: 10.1103/PhysRevB.76.144415 PACS number(s): 72.25.Dc, 75.47.−m, 75.50.Pp

I. INTRODUCTION

In the field of spintronics with semiconductors, the integration of the *p*-type ferromagnetic semiconductor (Ga,Mn)As in III-V heterojunctions has allowed us to study physical effects related to the injection of a spin-polarized tunneling current in the valence band of semiconductors. The complexity of the transport mechanisms associated with spin-orbit coupled states makes this material a powerful means for finding effects and provides challenges for theoretical understandings. This includes tunnel magnetoresistance (TMR) across single and double barriers[1,2] tunnel anisotropic magnetoresistance (TAMR),[3,4] Coulomb blockade anisotropic magnetoresistance,[5] and spin transfer experiments.[6,7] Nevertheless, one of the main limitation of such *p*-type material for spintronics integration is the relatively low Curie temperature. Through postgrowth low-temperature annealing treatment, Curie temperatures as high as 173 K could be obtained.[8] The elimination of interstitial manganese atoms, double donors, that couple antiferromagnetically with the manganese atoms in substitutional position is mainly invoked to explain the increase of the critical temperature. Such Mn atoms diffuse towards the surface to form either a MnO (Refs. 9 and 10) or a MnN (Ref. 11) layer, depending upon the annealing conditions.

In this paper we describe the effect of annealing on the magnetic and electric properties of a (Ga,Mn)As/(In,Ga)As/(Ga,Mn)As tunnel junction. We have focused our report on this single hetereojunction even though other structures of different Mn concentrations and of different thicknesses were studied, leading to the same general trends than those reported here.[12] In the first part, we detail the effect of annealing on magnetization measurements and confirm observations made on a (Ga,Mn)As trilayer structure with a GaAs barrier.[13] The second part presents the results obtained on junctions fabricated by optical lithography by describing the behavior of resistance area (*RA*) product, TMR, and TAMR through annealing. In the last part, a general interpretation of the data behavior from both magnetic and electric measurements is given through a 6×6 band $k\cdot p$ model of the tunneling transport. Two important parameters are clearly identified: the hole filling related to the position of the Fermi level, ϵ_F, and the spin splitting parameter, B_G, introduced in the framework of the Zener model through the mean-field approximation.[14]

II. EXPERIMENTAL RESULTS

The $Ga_{0.926}Mn_{0.074}As$ (80 nm)/$In_{0.25}Ga_{0.75}As$ (6 nm)/$Ga_{0.926}Mn_{0.074}As$ (15 nm) structure from the top to bottom was grown by molecular beam epitaxy at 250 °C on a *p*-doped GaAs buffer layer ($p\cong2\times10^{19}$ cm^{-3}). Annealing treatment has been performed at 250 °C in a nitrogen atmosphere during 1 h. Concerning the magnetic measurements, the annealing was performed on a whole piece of 5×5 mm^2 whereas it was realized on patterned junctions for electrical experiments.

Figure 1 displays the magnetization curve of the sample measured by superconducting quantum interference device before and after the annealing procedure. The two step magnetization reversal along [100] axis at 10 K originates from the consecutive reversal of the two magnetic layers [Fig. 1(a)]. From those measurements, one can extract three im-

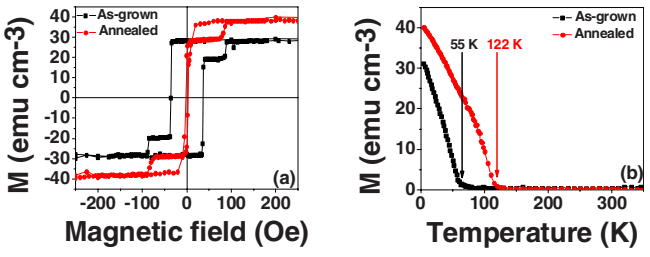

FIG. 1. (Color online) (a) Magnetization curve vs magnetic field at 10 K before and after annealing along [100] direction; (b) magnetization curve as a function of the temperature before and after annealing in a field of 500 Oe.

 ©2007 The American Physical Society

portant features consistent with the reduction, by the annealing procedure, of interstitial Mn in the top magnetic layer: a large decrease of the coercivity H_C, an increase of the magnetic moment M_S, as well as an increase of the Curie temperature T_C. Concerning the variation of H_C, previous magnetization study pointed out that the related decrease of the coercive field of a (Ga,Mn)As film should be associated with the elimination of pinning centers played by interstitial Mn.[15] The resulting increase of the carrier concentration may also contribute to the decrease of the anisotropy field as well as the increase of the average exchange interactions.[14] Derived from the mean-field theory, the average spin-splitting parameter within (Ga,Mn)As can be estimated from the saturation magnetization according to $B_G = \frac{A_F \beta M_S}{6 g \mu_B}$ where A_F is the Fermi liquid parameter and β the p-d exchange integral.[14] Considering that only the top (Ga,Mn)As layer is affected by thermal treatment, it is then possible to evaluate the increase of the spin-splitting B_G parameter from -17 to -24 meV by annealing.

The observed Curie temperatures are in good agreement with those found on thicker magnetic layers confirming that (Ga,Mn)As layers of width larger than 50 nm should still possess a large concentration of interstitial manganese.[10,16] In the present case, the Curie temperature goes from 55 to 122 K [Fig. 1(b)]. Because of the larger magnetic moment carried by the top layer, the behavior of the thin bottom layer is hidden in the full magnetization cycle, supporting the conclusion that only the properties of the top layer are modified. A further confirmation is provided by the Auger electron spectroscopy analysis of the chemical profile of Mn within the whole structure (not reported here). A significant Mn accumulation at the top of the surface is clearly evidenced, whereas no obvious change was observed in the bottom layer. This result was already put forward by Chiba *et al.*[13] It is known from Stoner *et al.*[17] that capping a (Ga,Mn)As film by a thin GaAs layer exceeding 5 nm does not improve its Curie temperature. The formation of a p-n junction avoiding the migration of interstitial n-type Mn was suggested.[18]

Magnetic tunnel junctions have been patterned by optical lithography (the junction size is ranging between 8 and 128 μm^2). The electrical measurements in the current perpendicular to plane regime were performed at 3 K and at low bias (1 mV) using standard dc technique. Nonlinear tunneling $I(V)$ curves recorded indicate that the 6 nm (In,Ga)As layer still acts as a barrier for holes injected from the (Ga,Mn)As source.[7] The reason is twofold: (i) the position of Mn acceptor level in the band gap of GaAs leads to an initial positive band offset between (Ga,Mn)As and GaAs and (ii) the incorporation of n-type As antisites during the low-temperature growth procedure governs, by part, the pinning of the Fermi level at a higher position in energy than expected neighboring the midgap of GaAs.

We are first going to address the TMR experiments. In Fig. 2(a), we note, for a 128 μm^2 junction, a conjugate increase of TMR from 30% to 120% after annealing associated with a decrease of the RA product (resistance $\times$ junction area at 3 K and 1 meV) from 0.05 to 0.003 Ω cm^2. Moreover, as already observed on magnetic properties and despite a discrepancy in magnitude related to size effects, the top magnetic layer is shown to be softened by annealing. Although the magnetic properties derive from the whole magnetic layers (volume effect) whereas the tunneling process is more sensitive to interfaces, it seems possible to draw some preliminary qualitative conclusions. Such observations, i.e., the lowering of the specific RA product and the reduction of the coercive field, has to be correlated to a change of the Fermi energy within (Ga,Mn)As involving, in parallel, an increase of the hole concentration as well as a reduction of the barrier height. Note, however, that no TMR bias asymmetry could be evidenced after annealing. This tends to prove that a homogenization of the carrier concentration takes place at both sides of the barrier due to the equalization of the Fermi level.

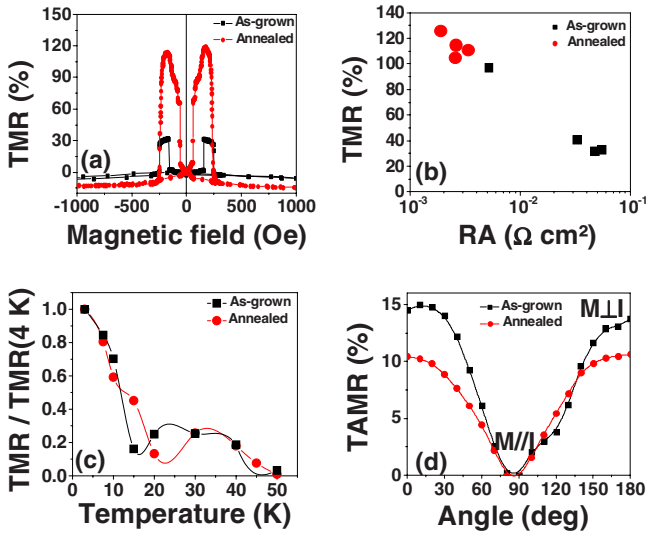

FIG. 2. (Color online) (a) Tunnel magnetoresistance measurements as a function of the magnetic field at 1 mV and 3 K for a 128 μm^2 junction. (b) Tunnel magnetoresistance measurements as a function of resistance $\times$ area product at 3 K for four (un)annealed junctions. (c) Tunnel magnetoresistance at 1 mV as a function of the temperature before and after annealing. (d) Tunnel anisotropic magnetoresistance measurements as a function of the orientation of a 6 kOe saturating field at 1 mV and 3 K for a 128 μm^2 junction. In the present case, 0° corresponds to an in-plane magnetization along [100] crystallographic direction and 90° to an out-of-plane magnetization along [001] crystallographic direction.

Some more general trends were observed on a set of four junctions [Fig. 2(b)]. Whereas TMR values shows a large discrepancy between 30% and 90% before annealing, a homogenization of the values occurs after annealing where TMR lays between 110% and 130%. Assuming spin-conservative tunneling transfer, the evolution of TMR with temperature has to be directly linked to the effective spin polarization of holes within the ferromagnetic layer.[19] Note that the effective temperature ($T \sim 55$ K) for which TMR vanishes remains unchanged after annealing [Fig. 2(c)]. This corresponds to the lower Curie temperature of the bottom electrode that was not affected by annealing. The drop of TMR around 15 K before and after annealing must be related to the rapid variation of the coercive field of the thin magnetic layer as a function of the temperature.[20]

We are now going to focus on TAMR measurements that reflect a variation of the tunnel RA product vs the crystallo-

graphic orientation of the magnetization in the saturation regime. In the present case, TAMR is mediated by the strong anisotropy of the (Ga,Mn)As valence band subject to both exchange and spin-orbit interactions. Concerning the experimental protocol, careful attention was paid to record the variation of the *RA* product when the magnetization, initially oriented in the plane along the [100] crystallographic direction, is rotated out-of-plane along the growth direction [001] in a saturating field of 6 kOe [Fig. 2(d)] giving maximal effects as follows:

$$\mathrm{TAMR}(\%) = 100 \times \frac{R_{[100]} - R_{[001]}}{R_{[001]}}.$$

A decrease of conductance of about 10–15% is thus evidenced at 3 K and 1 mV by rotating the magnetization in the direction of the tunneling current, in good agreement with experiments obtained with a ZnSe barrier.[4] The same behavior and range have been on the set of four junctions before and after annealing. No resistance variations higher than 4% could be detected when rotating the magnetization in the plane of the junctions.

III. THEORETICAL MODEL

Our calculations of the transmission coefficient are based on the multiband transfer matrix technique developed in detail by Pethukov *et al.*,[21] Brey *et al.*,[22] and Krstajic and Peeters[23] and applied to the hole 6×6 valence band $k\cdot p$ Hamiltonian H_h. Added to the Kohn-Luttinger kinetic Hamiltonian, this includes a p-d exchange term introduced by the interaction between the localized Mn magnetization and the holes derived in the mean-field approximation thus giving

$$H_h = -(\gamma_1 + 4\gamma_2)k^2 + 6\gamma_2 \sum_{\alpha} L_\alpha^2 k_\alpha^2 + 6\gamma_3 \sum_{\alpha\neq\beta} (L_\alpha L_\beta + L_\beta L_\alpha) k_\alpha k_\beta + \lambda_{so} \vec{L}\vec{S} + 6B_G \hat{m}\vec{S} \quad (1)$$

equivalent to the one proposed by Dietl *et al.*[14] and Abolfath *et al.*[24] Here, $\alpha=\{x,y,z\}$, L_α are $l=1$ angular momentum operators, $\vec{S}$ is the vectorial spin operator, $\hat{m}$ the unit magnetization vector, and γ_i are Luttinger parameters of the host semiconductor GaAs. $6B_G$ represents the spin splitting between the spin up and spin down heavy holes at the Γ_8 point like originally introduced by Dietl *et al.*[14] We did not take explicitly into account the stress Hamiltonian which is shown to give the same qualitative conclusions than the ones elaborated further.

To derive the transmission coefficient, the boundary conditions to match at each interface are[21] as follows.

(i) The continuity of the six components of the envelope function according to $\psi_n^+ + \Sigma_{\bar{n}} r_{n,\bar{n}} \psi_{\bar{n}}^- = \Sigma_{n'} t_{n,n'} \psi_{n'}^+$, where the subscript $t_{n,n'}$ ($r_{n,\bar{n}}$) refer to the respective transmission (reflection) amplitude from *incident* (n), *reflected* ($\bar{n}$), and *transmitted* (n') waves.

(ii) The continuity of the six components of the current wave vector according to $\hat{J}\psi_n^+ + \Sigma_{\bar{n}} r_{n,\bar{n}} \hat{J}\psi_{\bar{n}}^- = \Sigma_{n'} t_{n,n'} \hat{J}\psi_{n'}^+$, where, in the $k\cdot p$ approach, the current operator in the z direction writes $\hat{J} = \frac{1}{\hbar}\frac{\partial H_h}{\partial k_z}$.

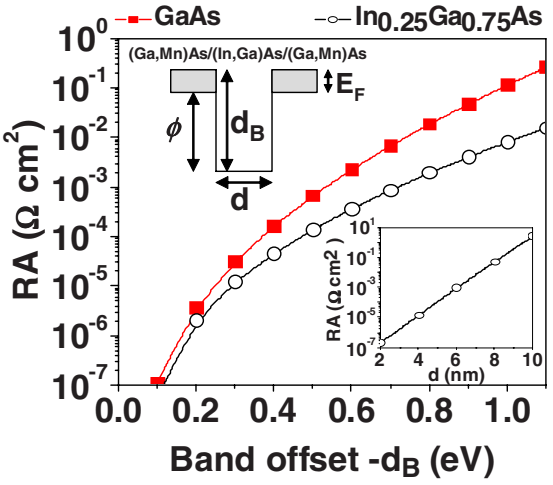

FIG. 3. (Color online) Calculated resistance area (*RA*) product of the trilayer structure as a function of the band offset d_B between the ferromagnetic semiconductor and a 6 nm barrier of GaAs or (In,Ga)As. The physical parameters used for (Ga,Mn)As are $6B_G=-120$ meV and $p=1.5\times10^{20}$ cm^{-3}. Insets: (bottom) *RA* product as a function of the (In,Ga)As barrier width d for a band offset $d_B=-0.7$ eV; (top) valence band profile of the heterojunctions.

Concerning the heterojunction itself, the valence band offset (VBO), d_B, between (Ga,Mn)As and (In,Ga)As fixes the effective barrier height ϕ according to $d_B=-\epsilon_F+\phi$ (inset of Fig. 3). The top of paramagnetic (Ga,Mn)As ($B_G=0$) valence band is taken here as the reference for energy. As an example, we present, on Fig. 3, the calculated *RA* product of a $(\mathrm{Ga,Mn})\mathrm{As}/\mathrm{In}_{0.25}\mathrm{Ga}_{0.75}\mathrm{As}(6\ \mathrm{nm})/(\mathrm{Ga,Mn})\mathrm{As}$ junction vs the respective VBO using standard Landauer formula for tunnel conductance. The physical parameters used for (Ga,Mn)As are $6B_G=-120$ meV and $p=1.5\times10^{20}$ cm^{-3} ($\epsilon_F\simeq-0.1$ eV) which seems quite reasonable. Although the VBO between $\mathrm{Ga}_{0.926}\mathrm{Mn}_{0.074}\mathrm{As}$ and $\mathrm{In}_{0.25}\mathrm{Ga}_{0.75}\mathrm{As}$ is still unknown, recent photoemission spectra determined the barrier height ϕ between (Ga,Mn)As and low-temperature grown (LT-grown) GaAs to be 0.45 eV.[25] This is in agreement with our $k\cdot p$ model considering a *RA* product approaching $\sim10^{-3}$ Ω cm^2 after annealing for $d_B=-0.55$ eV (Fig. 3) as well as with experimental results of Chiba *et al.*[20] To match with our calculation (Fig. 3), the valence band offset between $\mathrm{In}_{0.25}\mathrm{Ga}_{0.75}\mathrm{As}$ and (Ga,Mn)As should be taken larger, of the order of $d_B=-0.7$ eV giving an effective barrier height of 0.6 eV. However, the true band offset between $\mathrm{In}_{0.25}\mathrm{Ga}_{0.75}\mathrm{As}$ and GaAs grown at high temperature is known to be less than 50 meV.[26] Nevertheless, it should be noted that, in the present case of LT-growth procedure, the real value of ϕ should depend on the following.

(i) The nature and density of the dangling bonds at each interface promoted by the low-temperature growth procedure fixing the real valence band offset between two semiconductors.[27]

(ii) The local density and position in energy of ionized defects in the barrier such as As antisites which strongly influences the valence band bending within the whole heterojunction as well as the average barrier height.

However, surprisingly, we have noticed that TMR remains almost insensitive to the barrier height ϕ (not shown). Let us

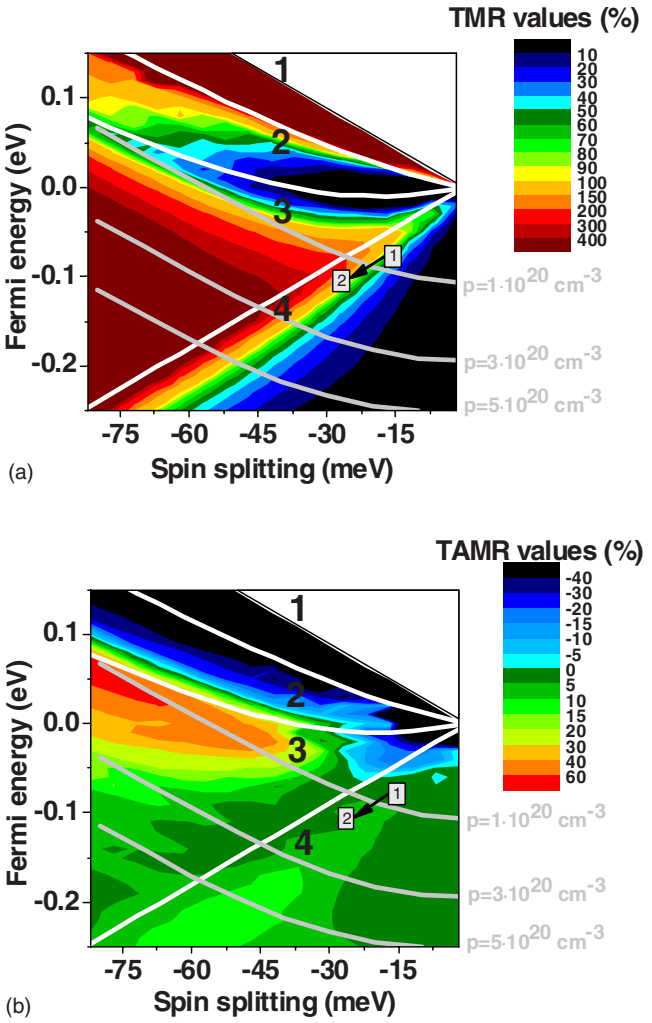

FIG. 4. (Color online) Tunnel magnetoresistance (a) and tunnel anisotropic magnetoresistance (b) vs Fermi energy and spin splitting for a 6 nm (In,Ga)As barrier and a band offset $d_B=-0.7$ eV. White lines represent the four bands at the center of the Brillouin zone. Gray lines indicate the Fermi energy for different hole concentrations.

then focus on the phase diagrams TMR (ϵ_F, B_G) and TAMR (ϵ_F, B_G) established from the previous model of $k\cdot p$ tunnel conduction. Figure 4 displays both TMR and TAMR vs the spin-splitting parameter B_G and the Fermi energy ϵ_F of the ferromagnetic semiconductor whose properties are assumed to be identical at both sides of the (In,Ga)As barrier. Also are plotted on phase diagrams three different lines corresponding to constant carrier concentrations of 1×10^{20}, 3.5×10^{20}, and 5×10^{20} cm^{-3}, as well as the energy of the four first bands at the center of the Brillouin zone. We are first going to discuss the general trends for TMR and TAMR from such diagrams.

IV. DISCUSSION

High TMR values, up to several hundred percents, can be expected either for spin-splitting values larger than several tens of meV or for low carrier concentration, that is, when only the first subband is involved in the tunneling transport. This corresponds to a quasi-half-metallic character for (Ga,Mn)As. Starting from the first subband and increasing the carrier concentration to fill the consecutive lower subbands ($n=2,3,4$), up and down spin populations start to mix up, leading to a decrease of TMR. For high carrier concentration ($n=4$), small TMR is expected which may anticipate difficulties to conciliate high Curie temperature and large TMR effects. We specify that for low values of spin splitting and Fermi energy, ferromagnetic phase induced by carrier delocalization may not exist (top right corner of the diagram), which is, of course, not taken into account in our $k\cdot p$ model using a basis of propagative envelope wave function. In the same manner, we cannot reproduce metal-insulator transition in the tunneling transport, responsible for the large in-plane TAMR.[3,28]

What about TAMR signal? We can first note a possible change of sign for TAMR on crossing the third subband. The first subband clearly gives a negative contribution to TAMR. This originates from the predominant heavy hole character of such band, an in-plane magnetization allowing, through off diagonal components, a possible heavy to light hole conversion, and then a larger transmission through the barrier.[29] This argument is reversed for the second and third subbands with the results that TAMR becomes positive when $n=2$ and $n=3$ subbands are dominant in the tunneling transport. We can point out that a change of TAMR sign was already observed on a Zener-Esaki diode[30] as well as theoretically established through tight-binding treatment.[31] Reducing the hole concentration through hydrogenation techniques gives the possibility to probe this possible crossover from positive to negative TAMR.[32] Concerning our experiments, taking into account conjugate TMR and TAMR values obtained before and after annealing, one can roughly evaluate the projection of the corresponding signals trajectories in the $[\epsilon_F, B_G]$ plane followed during annealing (Fig. 4). The Fermi energy is the free parameter and it is chosen to reproduce at best the amplitude of both the measured TMR [(Fig. 2(a)] and TAMR [Fig. 2(d)]. A good qualitative agreement can be found even though symmetrical junctions were simulated in order to restrict the number of parameters.

Evaluating directly the interfacial spin splitting from the mean-field theory appears difficult since the interfacial magnetic properties are hardly accessible. However, using the B_G value estimated in mean-field theory from the measured magnetic moment (before and after annealing), a good qualitative agreement can be found for TMR and TAMR, as illustrated by the trajectory represented on Fig. 4 between point 1 (before annealing) and point 2 (after annealing). A more refined calculation including two different B_G values after annealing should be required to draw definite quantitative conclusion.

We are now going to discuss the hole concentration derived from these diagrams. TMR and TAMR values obtained before annealing are well reproduced for a hole concentration approaching 10^{20} cm^{-3} (Fig. 4), in good agreement with the one measured for a single (Ga,Mn)As layer and already reported.[33] Indeed, lower hole concentrations involve negative TAMR values and higher hole concentrations involve very weak TMR values. The annealing procedure has for effect to (i) remove Mn interstitial atoms, (ii) increase carrier

concentration, and (iii) reduce the effective barrier height even if the valence band position is expected to grow up due to an increase of the average exchange energy (B_G). The strong reduction of the *RA* product associated with the increase of TMR is consistent with such assumption. Nevertheless, the hole concentration extracted after annealing from the phase diagram $\sim 1.7\times 10^{20}$ cm^{-3} appears to be weak compared to the one reported in the literature and derived from Hall effect measurements. The existence of a possible concentration gradient can be at the origin of such discrepancy. Also can be invoked a reduction of the hole concentration at the interfaces with the barrier due to a significant charge transfer between *p*-type (Ga,Mn)As and *n*-type (In,Ga)As (excess of As antisites).[28,34]

V. CONCLUSION

In summary we have shown that annealing a (Ga,Mn)As-based tunnel junction mainly affects the properties of the top magnetic layer, ensuring an increase of the effective magnetization and a significant enhancement of the tunnel magnetoresistance. The comparison between experiments and modelization of the spin-polarized tunneling current using 6×6 band $k\cdot p$ treatment vs intrinsic (Ga,Mn)As parameters (hole filling and exchange energy) allowed a rough estimation of the average exchange interactions and carrier concentration in (Ga,Mn)As at the interface with the barrier. We point out that while the magnitude of TMR appears very sensitive to both parameters (B_G and ϵ_F), the TAMR variation is limited to several tens of percent but may change sign crossing from upper to lower (Ga,Mn)As subbands. As a final conclusion, we think that this reduced parameter model gives a good qualitative agreement of the tunneling transport and enables us to extract the fundamentals of TMR and TAMR processes involving tunnel transport of spin-orbit couple state. In order to go further and draw more quantitative information, a perfect control and knowledge of the carrier density seems to be necessary.

ACKNOWLEDGMENTS

We gratefully acknowledge H.-J. Drouhin, A. Fert, G. Fishman, and B. Vinter for fruitful discussions. This work was supported by the EU Project NANOSPIN FP6-2002-IST-015728 and by the french ANR Program of Nanosciences and Nanotechnology (PNANO) project MOMES.

*marc.elsen@paris7.jussieu.fr
†jean-marie.george@thalesgroup.com

[1] M. Tanaka and Y. Higo, Phys. Rev. Lett. **87**, 026602 (2001).
[2] R. Mattana, J.-M. George, H. Jaffrès, F. N. van Dau, A. Fert, B. Lépine, A. Guivarc'h, and G. Jezequel, Phys. Rev. Lett. **90**, 166601 (2003).
[3] C. Ruster, C. Gould, T. Jungwirth, J. Sinova, G. M. Schott, R. Giraud, K. Brunner, G. Schmidt, and L. W. Molenkamp, Phys. Rev. Lett. **94**, 027203 (2005).
[4] H. Saito, S. Yuasa, and K. Ando, Phys. Rev. Lett. **95**, 086604 (2005).
[5] J. Wunderlich *et al.*, Phys. Rev. Lett. **97**, 077201 (2006).
[6] D. Chiba, Y. Sato, T. Kita, F. Matsukura, and H. Ohno, Phys. Rev. Lett. **93**, 216602 (2004).
[7] M. Elsen, O. Boulle, J.-M. George, H. Jaffrès, R. Mattana, V. Cros, A. Fert, A. Lemaitre, R. Giraud, and G. Faini, Phys. Rev. B **73**, 035303 (2006).
[8] K. Y. Wang, R. P. Campion, K. W. Edmonds, M. Sawicki, T. Dietl, C. T. Foxon, and B. Gallagher, *Proceedings of the 27th International Conference on Physics of Semiconductors*, edited by J. Menéndez and C. G. Van de Walle, AIP Conf. Proc. No. 772 (AIP, Melville, New York, 2005), p. 333.
[9] K. W. Edmonds *et al.*, Phys. Rev. Lett. **92**, 037201 (2004).
[10] K. M. Yu, W. Walukiewicz, T. Wojtowicz, I. Kurykiszyn, X. Liu, Y. Sasaki, and J. K. Furdyna, Phys. Rev. B **65**, 201303(R) (2002).
[11] B. J. Kirby, J. A. Borchers, J. J. Rhyne, S. G. E. te Velthuis, A. Hoffmann, K. V. O'Donovan, T. Wojtowicz, X. Liu, W. L. Lim, and J. K. Furdyna, Phys. Rev. B **69**, 081307(R) (2004).
[12] M. Elsen, Ph.D. thesis, Université Pierre et Marie Curie (Paris VI), 2007.
[13] D. Chiba, K. Takamura, F. Matsukura, and H. Ohno, Appl. Phys. Lett. **82**, 3020 (2003).
[14] T. Dietl, H. Ohno, and F. Matsukura, Phys. Rev. B **63**, 195205 (2001).
[15] S. J. Potashnik, K. C. Ku, R. F. Wang, M. B. Stone, N. Samarth, P. Schiffer, and S. H. Chun, J. Appl. Phys. **93**, 6784 (2003).
[16] K. M. Yu, W. Walukiewicz, T. Wojtowicz, W. L. Lim, X. Liu, U. Bindley, M. Dobrowolska, and J. K. Furdyna, Phys. Rev. B **68**, 041308(R) (2003).
[17] M. B. Stone, K. C. Ku, S. J. Potashnik, B. L. Sheu, N. Samarth, and P. Schiffer, Appl. Phys. Lett. **83**, 4568 (2003).
[18] B. J. Kirby, J. A. Borchers, J. J. Rhyne, K. V. O'Donovan, T. Wojtowicz, X. Liu, Z. Ge, S. Shen, and J. K. Furdyna, Appl. Phys. Lett. **86**, 072506 (2005).
[19] R. Mattana *et al.*, Phys. Rev. B **71**, 075206 (2005).
[20] D. Chiba, F. Matsukura, and H. Ohno, Physica E (Amsterdam) **21**, 966 (2004).
[21] A. G. Petukhov, A. N. Chantis, and D. O. Demchenko, Phys. Rev. Lett. **89**, 107205 (2002).
[22] L. Brey, C. Tejedor, and J. Fernandez-Rossier, Appl. Phys. Lett. **85**, 1996 (2004).
[23] P. Krstajic and F. M. Peeters, Phys. Rev. B **72**, 125350 (2005).
[24] M. Abolfath, T. Jungwirth, J. Brum, and A. H. MacDonald, Phys. Rev. B **63**, 054418 (2001).
[25] M. Adell, J. Adell, L. Ilver, J. Kanski, and J. Sadowski, Appl. Phys. Lett. **89**, 172509 (2006).
[26] S. Tiwari and D. J. Frank, Appl. Phys. Lett. **60**, 630 (1992). If one takes into account explicitely the stress between (Ga,Mn)As and (In,Ga)As, this shift should correspond to the valence band offset between (Ga,Mn)As and the lighthole component of (In-,Ga)As that is preferentially transmitted through thick barriers.
[27] S. Lodhaa, D. B. Janes, and N.-P. Chen, J. Appl. Phys. **93**, 2772 (2003).

[28] K. Pappert, M. J. Schmidt, S. Humpfner, C. Ruster, G. M. Schott, K. Brunner, C. Gould, G. Schmidt, and L. W. Molenkamp, Phys. Rev. Lett. **97**, 186402 (2006).
[29] M. Elsen, H. Jaffrès, R. Mattana, M. Tran, J.-M. George, A. Miard, and A. Lemaitre, Phys. Rev. Lett. **99**, 127203 (2007).
[30] R. Giraud, M. Gryglas, L. Thevenard, A. Lemaitre, and G. Faini, Appl. Phys. Lett. **87**, 242505 (2005).
[31] P. Sankowski, P. Kacman, J. A. Majewski, and T. Dietl, Phys. Rev. B **75**, 045306 (2007).
[32] L. Thevenard, L. Largeau, O. Mauguin, A. Lemaitre, and B. Theys, Appl. Phys. Lett. **87**, 182506 (2005).
[33] M. Malfait, J. Vanacken, W. V. Roy, G. Borghs, and V. Moshchalkov, J. Magn. Magn. Mater. **290**, 1387 (2005).
[34] A. Koeder *et al.*, Appl. Phys. Lett. **82**, 3278 (2003).